

## Nuclear central force in the chiral limit

John F. Donoghue

*Department of Physics, University of Massachusetts, Amherst, Massachusetts 01003, USA, and Institut des Hautes Études Scientifiques, Bures sur Yvette, F-91440, France*

(Received 8 March 2006; published 17 August 2006)

Chiral perturbation theory supplemented by the Omnes function is employed to study the strength of the isoscalar central nuclear interaction,  $G_S$ , in the chiral limit vs the physical case. A very large modification is seen, i.e.,  $\eta_s = G_{S\text{chiral}}/G_{S\text{physical}} = 1.37 \pm 0.10$ . This large effect is seen to arise dominantly at low energy from the extra contributions made by massless pions at energies near the physical threshold where the physical spectral function must vanish kinematically. The slope away from the chiral limit,  $d_S$ , is also calculated and is correspondingly large. I also explain why this large variation is to be expected.

DOI: [10.1103/PhysRevC.74.024002](https://doi.org/10.1103/PhysRevC.74.024002)

PACS number(s): 21.30.Fe, 12.39.Fe, 24.85.+p

### I. INTRODUCTION

For the most part, we have obtained so far only a phenomenological description of the nuclear force. Whether using meson exchange potentials or effective field theory, the parameters of the internucleon interaction are hard to relate directly to QCD. However, I will show that we know enough to understand the quark mass dependence of the nuclear central interaction with reasonable control. I will use this understanding to describe the strength of the nuclear interaction in the chiral limit. We will see that there exists a strong variation in the strength, which nevertheless comes from readily understandable physics.

The basic framework will use a dispersive representation for the scalar-isoscalar interaction. The overall strength will be governed by a contact interaction

$$H_{\text{contact}} = G_S \bar{N} N \bar{N} N + \dots \quad (1)$$

The strength of this interaction will be related to a dispersion relation [1,2]

$$G_S = \frac{2}{\pi} \int_{2m_\pi}^{\infty} \frac{d\mu}{\mu} \rho_S(\mu^2). \quad (2)$$

Here the spectral function in the integrand  $\rho_S(\mu)$  is to be calculated from physical intermediate states of two-pion exchange, using chiral amplitudes at low energy plus the Omnes function for pion rescattering. We can control the mass dependence of these ingredients to a great extent using chiral perturbation theory.

Let us at this stage show the basic result, to be developed more fully below. The spectral function for the physical case was developed in Ref. [3], where it was shown to reproduce the shape and magnitude expected from past experience with scalar exchange. This result, with a small modification to be described below, is shown in Fig. 1. Also shown is the result that will be developed for the spectral function in the chiral limit. The integral under these curves gives the strength of the scalar interaction.<sup>1</sup> The chiral limit is seen to have a

<sup>1</sup>The negative “peak” in this figure is phenomenologically equivalent to the exchange of a “ $\sigma$ ” resonance.

greater strength largely because the threshold extends down to zero energy and the spectral function develops quickly. As will be discussed more fully below, there is some modeling involved in producing these spectral functions, and there are some gaps in our understanding of mass effects. However, the bulk of the change in the chiral limit comes from relatively low energies, where we have better control over the calculation. These low energy effects are easy to defend as predictions of chiral perturbation theory.

These contact interactions enter modern descriptions of nuclear binding. They have been developed in a systematic fashion in the treatment of light nuclei. Below I will also discuss the modification in the binding energy in heavy nuclei using the contact interactions. We will find a large increase in the binding energy per nucleon.

In chiral perturbation theory, the coupling constants will have an expansion in the pion mass. The leading terms will be

$$G_S = G_{S0}(1 + d_S m_\pi^2) + F_S m_\pi^3 + \dots \quad (3)$$

Equivalently, one sees also the parameter  $D_S \equiv d_S G_S$  defined. I will use my results to generate a value for the chiral slope  $d_S$ .

The results indicate rather large shifts as one goes to the chiral limit. In particular, I will find

$$\eta_{S,\text{ch}} = \frac{G_S|_{\text{chiral}}}{G_S|_{\text{physical}}} = 1.37 \pm 0.10, \quad (4)$$

$$d_S = \frac{0.31 \pm 0.08}{m_\pi^2}.$$

When unexpectedly large effects are found, it is important to carefully understand their origin and assess whether the effects are reasonable. I spend considerable effort on this task in this paper, and we can in fact understand why a large effect is found.

In Sec. II, I describe some properties of effective field theory that make it reasonable that such a large mass variation exists. In Sec. III, the basic framework is displayed. Section IV discusses the leading chiral amplitudes for the spectral function. Section V describes the Omnes function and the framework that I use for approximating the phase shifts. Section VI puts these ingredients together and shows the comparison of the physical case to the chiral limit. I also

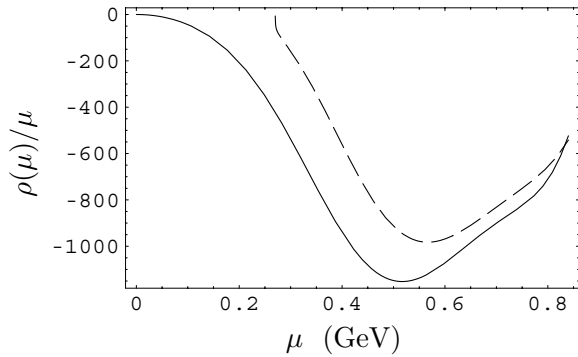


FIG. 1. Spectral integrand,  $\rho_S(\mu)/\mu$ , whose integral determines the strength of the scalar-isoscalar interaction. Solid line is for the chiral limit; dashed line is calculated with the physical pion mass.

discuss the uncertainties of the calculation here. Section VII uses this scalar coupling to describe nuclear binding in the chiral limit. The slope away from the chiral limit  $d_S$  is extracted in Sec. VIII. Finally, in Sec. IX, I briefly summarize the results and discuss the relation of this work to previous treatments of the nuclear force in the chiral limit [4–6].

## II. EFFECTIVE FIELD THEORY AND LOW-ENERGY EFFECTS

There is a dichotomy between the way that we describe the philosophy of effective field theory and the way that we implement it in practice. The difference is important to the understanding of the present problem. Let me introduce these notions through a simpler problem which is by now well understood, and which also has an anomalously large mass dependence, namely, pion and kaon electromagnetic mass splitting. I then show how this philosophy is relevant to the problem of the scalar interaction in nuclei.

An effective field theory is the description of the low-energy limit of a theory, with the correct degrees of freedom and interactions for the low-energy world. As originally explained by Wilson [7], we describe the low-energy interaction below some scale  $\Lambda$  by the propagation of the light degrees of freedom. The high-energy effects above the scale  $\Lambda$  are incorporated into a set of local Lagrangians. They must be local at energies  $E \ll \Lambda$  due to the uncertainty principle. We then have a clear way of separating low-energy effects, which we can readily calculate, from high-energy effects, which we often cannot calculate but can readily parametrize.

However, this is not how we generally proceed in practice. The use of a cutoff  $\Lambda$  to separate low energy from high energy is awkward. Energy cutoffs require care in order to not violate Lorentz invariance, gauge invariance, and/or chiral symmetry. In practice, we generally calculate using dimensional regularization. However, this scheme does not have a separation between low energy and high energy—all scales are integrated over in loop diagrams. This is not a problem in principle. Extra or missing contributions can be adjusted by a shift in the values of the contact interactions. However, and this will be our topic here, unexpectedly large

mass effects can occur if large *low-energy* contributions are put into the contact interaction.

Let us explore this first in the context of the pion electromagnetic mass difference. This is described by the chiral Lagrangian

$$\mathcal{L}_{EM} = g_{EM} \text{Tr}(QUQU^\dagger), \quad (5)$$

in usual notation. One consequence of this is the equality of the electromagnetic mass splitting of pions and kaons

$$(m_{\pi^+}^2 - m_{\pi^0}^2)_{EM} = (m_{K^+}^2 - m_{K^0}^2)_{EM}, \quad (6)$$

which is known as Dashen's theorem [8]. Normally, corrections to this would be expected to be of order 25% from the naive dimensional analysis estimate of SU(3) breaking due to quark mass differences. However, direct calculation of the mass differences in chiral-based models yields a 100% violation of Dashen's theorem [9]. The reason why the models are right and the naive dimensional analysis estimate is wrong has to do with the distinction described above.

In the effective field theory, the degrees of freedom are pions, kaons, and photons. In a Wilsonian effective field theory, the quantum effects of the light particles in the diagram of Fig. 2 should be calculated up to the scale  $\Lambda$ , and only the effects beyond that scale parametrized by the chiral Lagrangian with coefficient  $g_{EM}(\Lambda)$ . Thus, in a Wilsonian scheme, there would be two different contributions: a dynamical contribution of the actual  $\pi$ ,  $K$ ,  $\gamma$  loop diagrams up to the scale  $\Lambda$  and a parameter  $g_{EM}(\Lambda)$  describing the physics beyond the scale  $\Lambda$ . There will also be higher order terms in the Lagrangian with extra factors of the pion and kaon masses. While we expect only a modest variation in the chiral Lagrangian with quark mass—this is the real content of Dashen's theorem—there is no such guarantee for dynamical effects of the light particles.

In dimensional regularization, the structure is different. The photon loop in dimensional regularization has the form (for the pion self-energy)

$$\sim \frac{e^2}{16\pi^2} \frac{m_\pi^2}{d-4}. \quad (7)$$

The factor of  $m_\pi^2$  is forced by dimensional analysis; there is no other dimensional factor in the calculation. Because of this factor, the loop does not renormalize  $g_{EM}$ , but goes into the renormalization of a higher dimension term in the Lagrangian that has extra factors of  $m_\pi^2$  and  $m_K^2$ ; let us call this parameter  $g_{EM,m^2}$ . So in dimensional regularization, there is no residual dynamical loop contribution, and the analysis only involves the parameters of the chiral Lagrangian treated at tree level.

It is easy to demonstrate that the greatest contributions to the chiral coefficient  $g_{EM}$  come from low-energy, not high-energy, physics. There is a dispersive sum rule [10] for  $g_{EM}$ , or



FIG. 2. Photon loop that contributes to the pion and kaon electromagnetic mass differences.

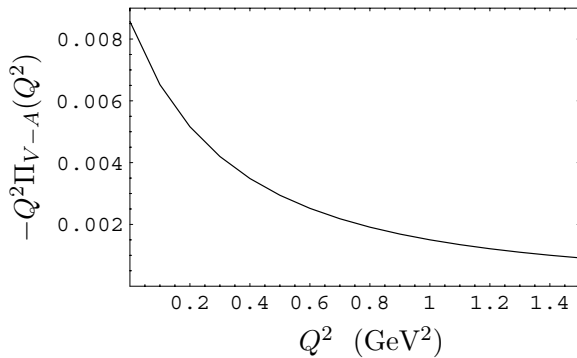


FIG. 3. Vacuum polarization function  $Q^2\Pi_{V-A}(Q^2)$  whose integral determines the chiral parameter  $g_{EM}$ . Notice that the greatest contribution comes from low energy.

equivalently the pion electromagnetic mass difference in the chiral limit, for which data exist. In the chiral limit, we have

$$g_{EM} = -\frac{3\alpha}{8\pi} \int_0^\infty dQ^2 Q^2 \Pi_{V-A}(Q^2), \quad (8)$$

where  $\Pi_{V-A}$  is the difference in the vector and axial-vector vacuum polarization functions.<sup>2</sup> In turn there is a spectral sum rule for  $\Pi_{V-A}$ , and the input to this sum rule can be obtained from  $\tau$  decay data. The integrand, derived from ALEPH data, is shown in Fig. 3. We see directly that most of the input comes from low energy.

Now consider what happens if we adopt the Wilsonian scheme and the dynamical low-energy contribution is relatively large. This dynamical effect can easily (and does) have over a 100% variation when comparing the pion with the kaon, because  $m_K^2 \sim 13m_\pi^2$  and we are in an energy region comparable to the masses. In this case, even if the mass dependence of short distance physics parametrized by the chiral Lagrangian is of normal size, the kaon mass shift can be very much different from that of the pion.

The Wilsonian approach is undoubtedly correct in saying that there is large SU(3) breaking at low energy. It is readily calculable using just the low-energy theory. However, when doing chiral perturbation theory in the usual fashion, regularized dimensionally, we would miss this effect. Dimensional regularization can accommodate this situation, but it is not the outcome that we would naively expect. It can be done only at the expense of having an anomalously large parameter in the chiral Lagrangian. The mass shift is described by  $g_{EM}$  and  $g_{EM,m^2}$ , which are *a priori* unknown. The latter must be taken to be much larger than naive expectation in order to reproduce the large difference.

What has happened is that in this scheme, important *low-energy physics* has been encoded in the parameter of the chiral Lagrangian  $g_{EM,m^2}$ . We normally expect that the chiral parameters are manifestations of only high-scale physics, but in a scheme like dimensional regularization, which does not have a separation between high and low scales, there can also be low-energy physics encoded in the parameters.

<sup>2</sup>There is an extensive literature on  $\Pi_{V-A}$ ; the figure is drawn from my own work on the subject [11].

The lesson from this is that if low-energy dynamical effects make a significant contribution to a process, there can be a large mass effect. This can lead to a larger-than-expected variation in chiral parameters when treated in the usual fashion. I will now argue that an analogous effect will occur in the parameter  $G_S$  describing the strength of the scalar interaction. That is, we will see that low-energy effects are embedded in this parameter and that these effects can have a very large variation.

Consider now the two-pion exchange contributions to the internucleon potential. The diagrams and formulas will be given later. In a Wilsonian approach, we would calculate explicitly the pionic effects up to some separation scale  $\Lambda$ , and then use a contact interaction  $G_S(\Lambda)$  to describe the high-energy effects beyond this scale. We might realistically expect that the mass effects in  $G_S(\Lambda)$  are modest. However, there can be no such expectations for the explicit two-pion calculation if there are significant contributions from energies around the pion mass. These contributions can vary by 100% as the pion mass is set to zero. For example, in Fig. 1 we see that the physical spectral function can only start at  $\mu = 2m_\pi$  while the chiral limit case extends down to zero energy. The two cases do not get close to each other until above 400 MeV, and the integrated values of the contribution below this energy are significantly different.

However, this Wilsonian approach is usually not carried out in practice. The interaction in the scalar channel is parametrized by a contact interaction (or  $\sigma$  potential) and the low-energy parts of the two-pion exchange are not separately evaluated. One calculates nuclear binding totally with the contact interaction or the potential. The consequence of this is that we should expect that the large mass variation of the dynamical two-pion exchange has to be included in the contact interaction, which then appears as if there were an anomalously large mass dependence of this coefficient. We see in Fig. 1 that the high-energy portion has a modest mass dependence, whereas the low-energy component has a 100% variation between the physical case and the chiral limit. If we were following the Wilsonian approach, the parameter  $G_S(\Lambda)$  would have a small mass variation if  $\Lambda$  were chosen above 500 MeV. However, in a usual calculation, the mass variation of  $G_S$ , encoded in the parameter  $d_S$ , must be taken to be very large in order to account for the low-energy effect. It is this which allows us to understand the large mass effect described in the following sections.

It should be said that there is now an attempt being made at what I call the Wilsonian approach. Epelbaum, Glöckle, and Meißner [12,13] have been calculating the pionic effects to the nuclear potential in chiral perturbation theory using a cutoff in the spectral integral. When supplemented with a cutoff dependent contact interaction, this is the procedure described above. It would be good to see this approach extended to the binding of heavy nuclei. It would be even preferable, without loss of generality, to use the Omnes formalism developed in the present paper for the low-energy amplitude, even if a cutoff is used. The Omnes function is a required feature of the full answer and tames the growing polynomial behavior of the chiral amplitudes such that there is not an excessive contribution from the energy region around the cutoff. This procedure is equally general because any mistake that is

introduced from the region around the cutoff can nevertheless be corrected for by an adjustment of the contact term.

### III. FORMALISM

Our procedure begins with the dispersion relation derived by Cottingham, Vinh Mau, and others [1,2]. For textbook reviews, see [14,15]. The scattering amplitude for two nucleons obeys an unsubtracted  $t$ -channel dispersion relation.

$$M(s, t) = \frac{1}{\pi} \int_{4m_\pi^2}^{\infty} d\mu^2 \frac{\text{Im}M(s, \mu^2)}{\mu^2 - t - i\epsilon}. \quad (9)$$

The imaginary part of this amplitude is connected to the crossed channel  $N\bar{N} \rightarrow N\bar{N}$  with the important intermediate state being that of two pions. The overall amplitude is decomposed into partial waves described by their spin and isospin quantum numbers. The greatest interest in this paper will be on the scalar-isoscalar ( $J = 0, I = 0$ ) channel. By taking the nonrelativistic limit and ignoring the energy dependence in the  $S$  channel, one can define a momentum space potential that depends only on the momentum transfer  $q^2$ . Using the scalar-isoscalar central potential as an example, let us define the corresponding spectral function

$$\rho_S(\mu) = \text{Im}V_S(q = i\mu). \quad (10)$$

In terms of this imaginary part, the potential is defined by the dispersion relation

$$V_S(q^2) = \frac{2}{\pi} \int_{2m_\pi}^{\infty} d\mu \mu \frac{\rho_S(\mu)}{\mu^2 + q^2}. \quad (11)$$

When converted to coordinate space, this defines an internucleon potential depending on the separation  $r$ , with a spectral representation

$$V_S(r) = \frac{1}{2\pi^2 r} \int_{2m_\pi}^{\infty} d\mu \mu e^{-\mu r} \rho_S(\mu). \quad (12)$$

For orientation, note that this description would produce the conventional  $\sigma$  exchange potential with the substitution

$$\rho_S(\mu) = -\pi g_\sigma^2 \delta(\mu^2 - m_\sigma^2). \quad (13)$$

This would recover the classic Yukawa potential in momentum and coordinate space:

$$V_\sigma = \frac{-g_\sigma^2}{q^2 + m_\sigma^2 - i\epsilon}, \quad (14)$$

and

$$V_S(r) = -\frac{g_\sigma^2}{4\pi r} e^{-m_\sigma r}. \quad (15)$$

However, the  $\delta$  function is not a good representation of the physics in the scalar channel. Instead, we will use chiral perturbation theory extended to higher energy with the Omnes representation to describe the ingredients to the scalar channel.

For all channels except that of one-pion exchange, the potential is short range, and in effective field theory, can be represented by a  $\delta$  function—a contact interaction. For

example, the scalar-and vector-isoscalar contact interactions would be represented as

$$H_{\text{contact}} = G_S \bar{N}N \bar{N}N + G_V \bar{N}\gamma_\mu N \bar{N}\gamma^\mu N + \dots \quad (16)$$

Since the Fourier transform of a constant is a  $\delta$  function, the contact interactions in coordinate space correspond to a constant in momentum space. These contact interactions are therefore given by the momentum space potential at  $q^2 = 0$ , i.e., for the scalar or vector channel,

$$G_{S,V} = V_{S,V}(q^2 = 0) = \frac{2}{\pi} \int_{(2m_\pi, 3m_\pi)}^{\infty} \frac{d\mu}{\mu} \rho_{S,V}(\mu^2). \quad (17)$$

Higher powers of momenta can be accommodated by derivative contact interactions. For the exchange of a narrow resonance, the contact interaction has the form  $G_i = \pm g^2/m_i^2$ , and I will use this relation for the vector meson effect.<sup>3</sup> However, for the scalar interaction it is important to have a more complete evaluation, as described below.

### IV. CHIRAL AMPLITUDES

The application of chiral perturbation theory to the nuclear force has an extensive literature; for reviews and references, see [13,17–20]. The pathway using the dispersion relation and the spectral function has been pioneered by Kaiser, Meißner, and collaborators [12,21–23]. We will find this a very effective description of nature of energy expansion for the nuclear interaction.

The low-energy behaviors of the two-pion-exchange diagrams have been calculated in perturbation theory. The  $\pi NN$  vertex is proportional to the axial charge  $g_A$ , and the two-pion vertices are parametrized by low-energy constants  $c_1, c_2, c_3$ , and  $c_4$  in the chiral Lagrangian. The diagrams are shown in Fig. 4. The diagrams of Figs. 4(a) and 4(b) lead to

<sup>3</sup>For resonance saturation estimates of these and other nuclear contact interactions, see [16].

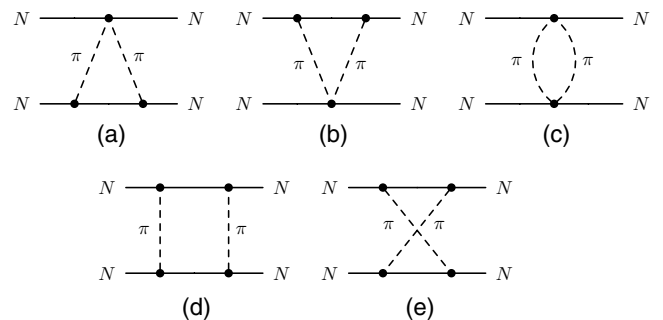


FIG. 4. Two-pion-exchange diagrams which arise in chiral perturbation theory.

the spectral function [21]<sup>4</sup>

$$\begin{aligned} \rho_S^{a,b}(\mu) = & \frac{3g_A^2}{64F_\pi^4} [4c_1 m_\pi^2 + c_3(\mu^2 - 2m_\pi^2)] \\ & \times \frac{(\mu^2 - 2m_\pi^2)}{\mu} \theta(\mu - 2m_\pi) \frac{4m_N}{\pi \sqrt{4m_N^2 - \mu^2}} \\ & \times \arctan \frac{\sqrt{(\mu^2 - 4m_\pi^2)(4m_N - \mu^2)}}{\mu^2 - 2m_\pi^2}. \end{aligned} \quad (18)$$

The result of [21] was calculated in the heavy baryon limit, and I have modified their result to include the effects of a finite nucleon mass [24], see also [25]. The difference is minor numerically. Diagram 4(b) is one power higher in the energy expansion and involves two factors of the low-energy constants  $c_{1,2,3}$ . The imaginary part of this diagram is [22]

$$\begin{aligned} \rho_S^c(\mu) = & -\frac{3}{32\pi F_\pi^4} \sqrt{1 - \frac{4m_\pi^2}{\mu^2}} \theta(\mu - 2m_\pi) \\ & \times \left( \left[ 4c_1 m_\pi^2 + \frac{c_2}{6} (\mu^2 - 4m_\pi^2) + c_3 (\mu^2 - 2m_\pi^2) \right]^2 \right. \\ & \left. + \frac{c_2^2}{45} (\mu^2 - 4m_\pi^2)^2 \right). \end{aligned} \quad (19)$$

In a proper effective field theory treatment, the box and cross box diagrams, Figs. 4(d) and 4(e), should not be included in the contact interaction. This is because one includes the pion as an explicit light degree of freedom and includes the  $\pi NN$  vertex in the low-energy Lagrangian treating pion exchange dynamically. In this framework, we have the Lagrangian consisting of the pionic interactions and a set of contact interactions. Using this framework, one includes loop diagrams, and the box diagrams emerge as dynamical effects in addition to the effects of the contact interaction. Therefore, in principle, the correct treatment is to treat the box and cross box separately from the contact interaction.<sup>5</sup> The box diagrams are finite and their short distance components are small. They do not contribute to the renormalization of the contact interaction. Because of this separation of dynamical pionic effects and the contact interaction in effective field theory treatments, I do not include the box diagrams in the calculation of the contact interaction.

On a purely practical level, these terms are small compared to the effects that we do study, at least for the scalar central potential. This is demonstrated in [21] and can also be seen in Fig. 3.15 of Ref. [15]. As an explicit example, if we take the  $q^2 = 0$  limit of the potential from these diagrams quoted

<sup>4</sup>Watch out for a sign difference; their momentum space potential has the opposite sign of the conventions used in the present paper.

<sup>5</sup>In fact, following the discussion of Sec. II, it would even be preferable to separate out the low-energy portions of the remaining diagrams and treat them dynamically, reserving the contact interaction for the short-distance part of the diagrams. This is the Wilsonian point of view. However, it is not standard practice, and so we include all of the diagrams in Figs. 4(a)–4(c) in the contact interaction.

in [21], one finds that they generate a shift in the nonanalytic mass correction of size

$$\Delta G_S = -\frac{15g_A^4 m_\pi^3}{1024\pi F_\pi^4 M} = 0.42 \text{ GeV}^{-2}, \quad (20)$$

where the total result is  $G_S \sim -400 \text{ GeV}^{-2}$ .

In practice, a variety of approximate methods treat the effects of the nuclear potential, especially for heavier nuclei. These methods may vary in how much of the box diagram effects are calculated dynamically. It is not always clear then how these approximation schemes map onto effective field theory. However, in Sec. VIII, I discuss results on binding using a scheme that does attempt to match the effective field theory treatment [26]. This uses a relativistic treatment, including full relativistic propagators for the pion and the nucleons, which does separate the pion from the contact interaction. While recognizing that the application of this framework to nuclear binding is an approximation method, it seems most appropriate to use the above constitution of the contact interaction when discussing this scheme.

## V. UNITARITY AND THE OMNES FUNCTION

A key ingredient in the present method is the use of the Omnes function, which incorporates the physical effects of pion rescattering [27]. This ingredient is not optional—it is required by unitarity. Moreover, the general form of the result is well known within the elastic region. The amplitude must have the form of a polynomial in the energy times the Omnes function

$$\Omega(\mu) = \exp \left[ \frac{\mu^2}{\pi} \int \frac{ds}{s} \frac{\delta(s)}{s - \mu^2} \right]. \quad (21)$$

Here  $\delta$  is the  $\pi\pi$  scattering phase shift, in our case for the  $I = 0, J = 0$  channel. Chiral perturbation theory is consistent with this order by order in the energy expansion. Following Ref. [28], we know how to match this general description to the results of chiral perturbation theory by appropriately identifying the polynomial.

The two-pion vertices that appear in Figs. 4(a)–4(c) are modified by this Omnes function in a way that is strictly analogous to the two-pion vertex described in [28]. In particular, as described in [3] the inclusion of the Omnes function means that the spectral function is given by

$$\rho_S(\mu) = \rho_S^{a,b} \text{Re}\Omega(\mu) + \rho_S^c |\Omega(\mu)|^2. \quad (22)$$

In chiral perturbation theory, there will be higher order modifications to each term. However, experience has shown that using the lowest order amplitudes supplemented by the Omnes function gives reasonably good results up to 700–800 MeV. I have applied this formalism to the nuclear central potential using the physical phase shifts matched to the lowest order results in order to generate the spectral function [3]. The result is very encouraging because it generates the main features known phenomenologically for this interaction. It was shown that this gives good results for the shape and magnitude of the spectral function in the scalar channel. In both the physical case and in the chiral limit (described below)

I have also tested the formalism under the inclusion of expected higher order interactions, and the general features of the results seem to be robust. I will use this representation of the spectral function in the applications below.

We have recorded the chiral amplitudes in the previous section. The task now is to understand how these amplitudes vary between the physical case and the chiral limit. There will be several ingredients that need to be explored. Some mass dependence is explicit in the chiral amplitudes. Other dependence is contained in the parameters  $F_\pi g_A$ . Finally, there is mass dependence in the Omnès function, or equivalently in the  $\pi\pi$  phase shifts. This latter feature requires the most work, and I will address it first.

At low momentum, we have explicit expressions for the  $\pi\pi$  scattering amplitudes through the work of Gasser and Leutwyler [29]. At higher energies, our best knowledge comes from a treatment that combines chiral symmetry, dispersion relations, crossing, and experimental data by Colangelo, Gasser, and Leutwyler (CGL) [30]. In [3] I used the CGL phase shifts to construct the Omnès function. However, because of the reliance on experimental data, we do not directly have the ability to vary the quark mass in this analysis. To calculate the Omnès function for the chiral limit, we need to introduce a method to model the high-energy behavior of the  $\pi\pi$  phase shifts in such a way that we can vary the pion mass.

There exists a good and successful method for extending the description of the chiral amplitudes, often referred to as the Padé approximation or the inverse amplitude method (IAM) [31,32]. This provides an analytic approximation to the scattering amplitudes in a form that fully satisfies unitarity and which can be matched order by order to the results of chiral perturbation theory. Matched to the results at order  $E^4$ , the result for the  $I = 0, J = 0$  amplitude is

$$T_{00} = t_2 + t_4 + \dots \rightarrow \frac{t_2^2}{t_2 - t_4}. \quad (23)$$

The second term  $t_4$  contains the effects of loop diagrams and hence also has imaginary parts. The beauty of the IAM representation is that this simple rearrangement allows the amplitude to satisfy unitarity exactly. While the method necessarily differs from the full answer beyond the order to which it has been matched,<sup>6</sup> studies have shown that this representation provides a good description of the scattering amplitudes up to reasonably large energies. For example, the scalar-isoscalar IAM amplitude is compared to the physical result of CGL in Fig. 5. The description is quite good up to 700 MeV, after which it falls short. The resulting Omnès function is also compared to that derived from the CGL phase shifts in Fig. 6.<sup>7</sup> Again, the results are similar, except at high energies, where the Omnès function is small.

<sup>6</sup>For example, some two-loop logarithms are missing when the IAM is matched at one loop order [33].

<sup>7</sup>In producing the Omnès function, I had to extend the phase shifts above the  $\mu = 850$  MeV endpoint of the CGL analysis so that the principle value part of the Omnès function integral would be well behaved near the upper end. Likewise in the IAM formalism, there is a corresponding extension. As long as this extension is smooth, it has little effect on this calculation.

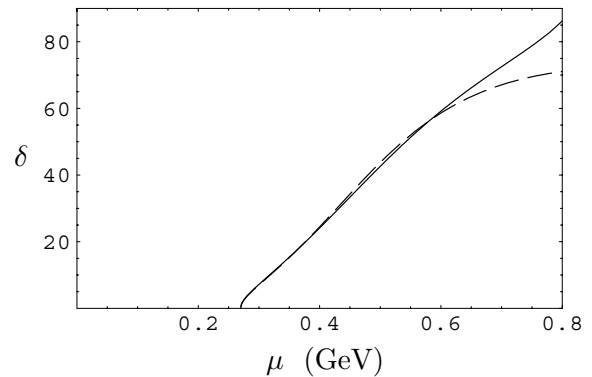


FIG. 5.  $\pi\pi$  phase shift from CGL (solid line) and from the inverse amplitude method (dashed line). Agreement is excellent up to about 700 MeV.

I will use the IAM phase shifts as an analytic approximation of the true amplitudes, keeping in mind the shortcomings at higher energies. The low-energy behavior of these phase shifts will then be fully rigorous, and the high-energy portion will be approximate.

Let us immediately look at the phase shift and the Omnès function in the chiral limit. The phase is shown in Fig. 7 in comparison with the IAM approximation to the physical case. The salient feature is the threshold behavior. The phase shift in the chiral limit clearly extends down to  $s = 0$ , and since this is the  $S$  wave, the strength turns on relatively quickly. The physical case needs to vanish at the physical threshold. These requirements naturally yield a larger phase shift for the chiral case throughout much of the physical region. At high energies, we see a much smaller difference between the chiral limit and the physical case. This is what should be expected, as the pion mass should make less of a difference at the higher energies. The Omnès function follows directly from the phase shifts and also has recognizable features. This is shown in Fig. 8.

These results are encouraging for the reliability of the method. The place where we have the least theoretical control is the upper energy end of the energy region. The IAM does not produce much variation at these energies, so most of the variation that we find comes from physics at lower energies. Moreover, the phase shifts only enter our calculation through the Omnès function, and the Omnès function is small at high energy. The true Omnès function from the CGL phase shifts is yet smaller, so the IAM slightly overemphasizes the higher energies. However, since there is not much mass variation at these energies, this is not a serious flaw. Overall, despite the approximate nature of the IAM method, there is no reason to doubt the general features of the resulting phase shift and hence the Omnès function.

## VI. DISPERSIVE CHIRAL ANALYSIS

In this section, the evaluation of the contact interaction will be presented. The key features of the scalar channel (i.e. the  $\sigma$ ) emerge, as reported in [3]. Moreover, the chiral limit will induce a shift in the scalar coupling that again emerges mostly from low energy two-pion exchange. In performing this

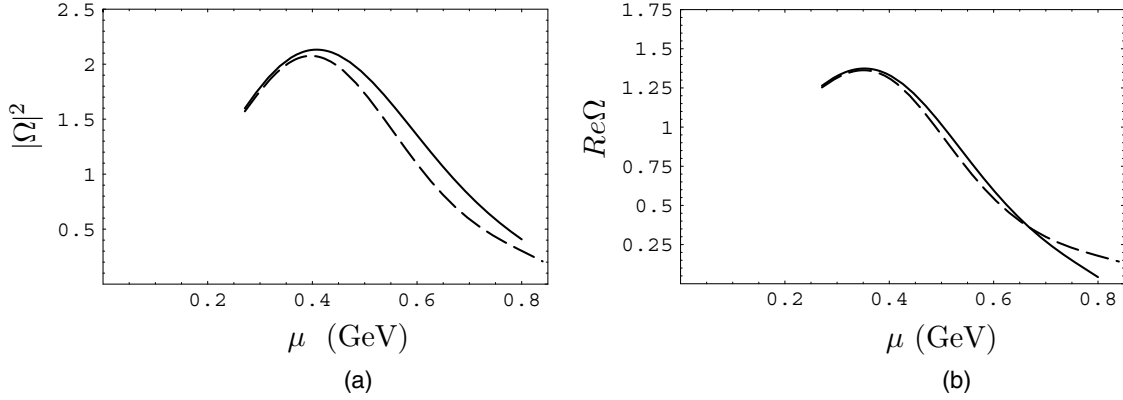


FIG. 6. Absolute square (a) and real part (b) of the Omnes functions derived from the CGL phase shifts (solid line) and those found using the inverse amplitude method (dashed line).

comparison, I have not varied the strange quark mass, keeping it fixed at its physical value.

In addition to the explicit dependence on the pion mass in the chiral amplitudes and the Omnes function, there is also implicit dependence on the pion mass contained in the parameters  $g_A$  and  $F_\pi$ . The dependence has the form [29,34]

$$F_\pi = F_0 \left[ 1 - \frac{1}{16\pi^2 F_0^2} m_\pi^2 \left( \ln \frac{m_\pi^2}{m_{ph}^2} + \bar{l}_4 \right) \right] \quad (24)$$

$$g_A = g_0 \left[ 1 - \frac{2g_0^2 + 1}{16\pi^2 F_0^2} m_\pi^2 \ln \frac{m_\pi^2}{m_{ph}^2} - \frac{g_0^2 m_\pi^2}{16\pi^2 F_0^2} + \frac{4m_\pi^2 \bar{d}_{16}}{g_0} \right]$$

with  $\bar{l}_4 = 4.4 \pm 0.2$  and  $\bar{d}_{16} = -1.0 \pm 0.7$ . While the mass dependence of the pion decay constant is fairly well constrained, the corresponding result in  $g_A$  is less well understood. This will be a significant component of our final error estimate.

The chiral parameters  $c_{1,2,3}$  are determined from a chiral analysis of pion-nucleon scattering [6,35,36]. When used without matching to the Omnes function at second order in  $m_\pi^2$ , as is the case both in the  $\pi N$  analyses and in this

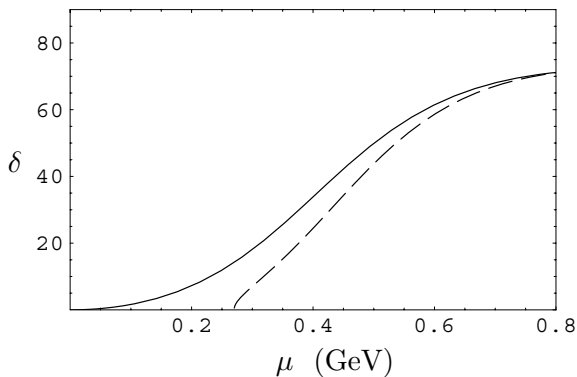


FIG. 7. Scalar-isoscalar  $\pi\pi$  phase shifts using IAM in the physical case (dashed line) and in the chiral limit (solid line).

paper, there is an ambiguity as to whether the fitted parameter should be identified with  $c_3$  itself or  $c_3\Omega(2m_\pi)$ , which is the threshold value of the coupling. Since  $\Omega(2m_\pi) \sim 1.25$ , this makes a difference in the result. The spectral function is dominantly determined by the parameter  $c_3$ , which, however, is not very well determined, with  $c_3 = -4.7^{+1.2}_{-1.0} \text{ GeV}^{-2}$  being the quoted value. If we used instead the constraint  $c_3\Omega(2m_\pi) = -4.7^{+1.2}_{-1.0} \text{ GeV}^{-2}$ , we would choose  $c_3 = -3.7^{+1.0}_{-0.8}$ . The overall magnitude of  $G_S$  does depend sensitively on the choice of  $c_3$ , see [3]. However, the ratio of  $G_S$  in the chiral limit to that of the physical limit is almost completely insensitive to  $c_3$ , as will be commented on below. Therefore, I will only quote the ratio as my final result. Although I have explored a wide range of  $c_3$  values, the figures were produced using  $c_3 = -4.0 \text{ GeV}^{-2}$ , a result intermediate between the two choices mentioned above and consistent with both within errors. The other parameter choices used were  $c_1 = -0.64 \text{ GeV}^{-2}$  [i.e.,  $c_1\Omega(2m_\pi) = -0.8$ ], and  $c_2 = 3.3 \text{ GeV}^{-2}$ . I explored the sensitivity of the results to these parameters, and both the magnitude and the ratio are insensitive to reasonable variations.

At this stage, we can put the pieces together. The chiral amplitudes of Eq. (22) contain both explicit and implicit mass dependence, as displayed above. The Omnes function has further dependence. The resulting integrand in the spectral sum rule for  $G_S$  was previously shown in Fig. 1, both for the physical case and for the chiral limit.

As described in [3], the shape of the spectral function in the physical case provides a reasonable representation of the  $\sigma$  that traditionally appears in the nuclear potential. Moreover, for reasonable values of the chiral parameters, in particular  $c_3$  which has the greatest impact, the physical value of  $G_S$  can be reproduced.

In traditional treatments of the nuclear interaction, the shape of the attractive isoscalar is described by a broad low mass  $\sigma$  particle near the mass of  $m_\sigma = 600 \text{ MeV}$ . The  $\sigma$  is not easily understood in terms of the quark and gluon degrees of freedom of QCD. It is unlikely that such a resonance is a traditional resonance in the spectrum of QCD. The  $\pi\pi$  phase shift is only about  $60^\circ$  at this mass, and does not pass through  $90^\circ$  anywhere in this neighborhood. A careful analysis [37] of the data and theory of  $\pi\pi$  scattering reveals a pole in the complex plane

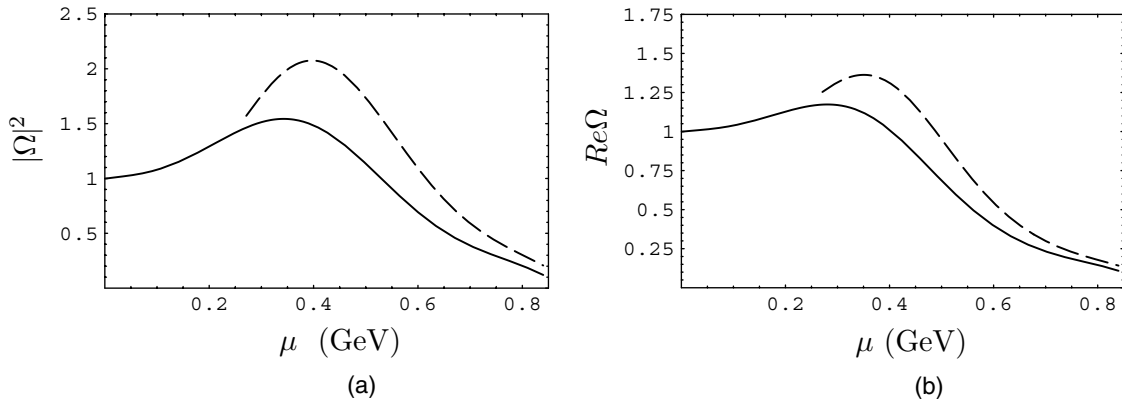


FIG. 8. Absolute square (a) and real part (b) of the Omnes functions in the physical case (dashed line) and in the chiral limit (solid line).

very far from the real axis, with mass  $\sim 440$  MeV and a larger width  $\Gamma \sim 540$  MeV. However, it is important to realize that the existence of this pole is not the determining feature for pionic interactions at this energy. The  $\pi\pi$  amplitudes are determined by the chiral expansion which is still well behaved when treated to one loop order at these energies. This amplitude is specified in terms of the pion decay constant and a pair of low-energy constants in the chiral lagrangian. These constants in turn are known to be determined by the properties of the  $\rho$  meson—there is no need or evidence of the  $\sigma$ . The existence of the distant  $\sigma$  pole plays little role in the structure of the  $\pi\pi$  amplitude in the 400–600 MeV energy range. In QCD, one can also see that the  $\sigma$  generated in the  $\pi\pi$  amplitude is not a fundamental resonance by an application of the large  $N_c$  rules [32]. Real resonances have a smooth result in the limit  $N_c \rightarrow \infty$ . However, scattering amplitudes vanish in this limit, and the  $\sigma$  found in the pion scattering amplitude disappears in the large  $N_c$  limit.

In the present treatment of the internucleon force, the effect that is traditionally described by a  $\sigma$  is reproduced even though the amplitude is not really described by the exchange of a scalar meson. The effect of the Omnes function is to reshape the spectral function so that it mimics a  $\sigma$ . The amplitude rises with increasing energy due to the energy dependence of the chiral amplitudes, but eventually turns over due to the addition of the Omnes function. The amplitudes could not continue to rise, otherwise unitarity would be violated. The Omnes function necessarily stops the growth of the chiral amplitudes and in practice ends up reproducing an energy dependence that mimics the form of a broad resonance. It should be noted that since the Omnes formalism uses the experimental  $\pi\pi$  phase shifts in the elastic region, there must also exist in this formalism the same pole far from the real axis that one finds in the  $\pi\pi$  analysis. However, again, this distant pole is not what determines the structure of the amplitude along the real axis. The chiral amplitudes along with the (nonresonant) phase shifts are the only important ingredients in this description. Even though the amplitude is not conventionally resonant at 500–600 MeV, the broad peaking of the spectral function reproduces an effect very similar to a  $\sigma$  resonance. Note that the use of the Omnes function is rigorous, and it can be matched to chiral perturbation theory to any given order.

The approximation of the present paper is the use of only the lowest order amplitudes as the polynomial that multiplies the Omnes function. These are fully rigorous at low energies, but are an approximate model when applied at higher energies.

It is, of course, not new to suggest that the  $\sigma$  effect is really a manifestation of two-pion exchange. In early work which extracted the internucleon potential from scattering data [1,2], it was clear that the lowest energy state contributing the spectral function in this channel had to be that of two pions, and hence the dynamics of  $\pi\pi$  exchange was crucial to the strength of the central interaction. Previous studies have discussed two-pion exchange in this channel (see [1,2,38–43] and references cited therein) as well as attempts to understand the  $\sigma$  in terms of quark degrees of freedom [44,45]. What is new in the present work is the ability to match the chiral perturbation theory treatment, the simplicity of the result, and the ability to have reasonable control over the mass dependence of the individual components of the formalism.

Since we have analytic control over the ingredients of this calculation, we may use this formalism to take the pion mass to zero. The result in the chiral limit has a similar high-energy behavior, and the magnitude there is only slightly increased. What is most striking is the enhancement at low energy. Much of this is purely kinematic. The threshold in the chiral limit extends down to zero energy, and the chiral predictions for the spectral function develop quickly.

To calculate the ratio of the scalar strength in the chiral limit to the physical limit, one compares the integral under the two curves in Fig. 1. The extra weight under the spectral integrand causes the value of  $G_S$  to increase significantly. Overall, I find that

$$\eta_{S,\text{ch}} \equiv \frac{G_S|_{\text{chiral}}}{G_S|_{\text{physical}}} = 1.37. \quad (25)$$

This is our primary result. It will be applied to the nuclear interaction in a subsequent section.

Let me attempt to assess the uncertainties in this result. Clearly, this calculation is not straight chiral perturbation theory, and hence it does not share the rigor of that method. I have modeled the moderate-energy behavior in the dispersive sum rule, and neglected all truly high-energy effects beyond 1 GeV. We clearly have no control over the effects at very high energy. However, there is no indication either phenomenologically or



theoretically that they are very important in the determination of  $G_S$ , nor that they would have significant dependence on the pion mass. We can look at the low- and moderate-energy uncertainties in more detail.

Most of the the shift in the scalar coupling comes from the low-energy region. The threshold behavior is an unambiguous feature—the chiral limit amplitudes must extend down to zero energy, and the chiral expansion becomes exact there. Even at moderate energies, the IAM representation of the pion phase shifts should be quite good. The greatest uncertainty in this region is the lack of understanding of the chiral behavior in the pion coupling to nucleons, as the leading spectral representation at low energy has a factor of  $g_A^2$ . This effect is quantifiable. The uncertainty in the chiral parameters  $d_{16}$  and  $\bar{l}_4$  corresponds to an uncertainty of  $\pm 0.07$  in our final result. Perhaps this uncertainty may be reduced in the future by lattice calculations. There could be additional  $m_\pi^2/(1\text{GeV})^2 \sim 0.02$  corrections to the  $c_{1,2,3}$  vertices besides those modeled by the Omnes factor, so there are clearly other uncertainties on the order of several percent.

The overall strength of  $G_S$  depends most heavily on the chiral parameter  $c_3$ . However, the ratio of the chiral limit to the physical case has only a remarkably tiny variation with this parameter. Throughout the whole range of  $c_3$  considered above, we find the ratio changes by less than 1%. Thus, the uncertainty due to the magnitude of this parameter is insignificant compared to other uncertainties.

One might worry that the treatment of two-pion exchange as a potential, or the use of a contact interaction instead of a potential, would break down in the chiral limit because of the massless pions. This could be the case if the very long range tail of the potential was significantly modified. Within this calculation, there is no evidence of a problem. The spectral function also can be used to predict a spatial potential  $V(r)$ . The physical result and the chiral limit result are shown in Fig. 9. The shape of the chiral result is quite similar to the physical limit.

The moderate-energy effects beyond the realm of straight chiral perturbation theory are less quantifiable, but we have reason to believe that they are not large. In contrast to the low-energy effects, there is no reason to expect that these effects are enhanced over the usual expectation of being of order  $m_\pi^2/\Lambda^2$ . Indeed, we find a reasonably small shift in the

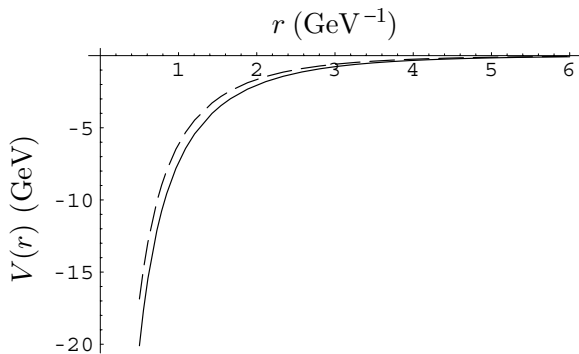


FIG. 9. Attractive scalar-isoscalar potential in the physical case (dashed line) and in the chiral limit (solid line).

spectral function at high energy, so our explicit calculation is consistent with this. However, I find it hard to defend that high-energy shift as a solid prediction of the method. If I were to neglect all shifts above 500 MeV, the main result for  $\eta_S$  would be about 5% smaller.

We can perform a further test by adding some expected higher energy effects. One uncertainty that we are able to explore numerically involves the energy dependence of the pion vertices. The two-pion vertex would presumably have some form factor associated with the leading coupling,  $c_3$ , which would generate a dependence of the vertex on the momentum transfer. I have studied this by creating an energy-dependent vertex through the substitution

$$c_3 \rightarrow \frac{c_3}{(\mu^2 + m^2)^n}. \quad (26)$$

As mentioned in [3], this modifies the shape of the spectral function somewhat and changes the integral that determines  $G_S$ . However, the change is modest enough that the desired value can still be obtained by changing the fit value of  $c_3$  within the allowed range. In this case, there is a modest increase in the chiral/physical ratio of  $G_S$ . For example, with  $n = 1$  and  $m = 1200$  MeV, there is a 29% decrease in the predicted value of  $G_S$  at fixed  $c_3$ . However, for the ratio  $\eta_{S,\text{ch}}$  this amounts to a 7% increase leading to the result  $\eta_{S,\text{ch}} = 1.46$ . The decrease in  $G_S$  and increase in  $\eta_S$  is readily understood. The form factor will decrease the contribution at higher values of  $\mu$ , but leave unchanged the threshold effects at small  $\mu$ . The former feature will decrease the physical value of  $G_S$ , but the new ingredients enhancing the chiral limit will be unchanged.

Additionally, in the section describing the chiral slope below, I will mention a puzzle concerning the lack of understanding of the nonanalytic behavior. While it is numerically small, this is also a feature that must somehow be generated from the higher energy portion of the spectral function.

I would summarize this discussion of the uncertainties by giving a final result of

$$\eta_{S,\text{ch}} \equiv \frac{G_S|_{\text{chiral}}}{G_S|_{\text{physical}}} = 1.37 \pm 0.10. \quad (27)$$

## VII. THE VECTOR CHANNEL

Also contributing to the central force is the dispersive channel involving three pions in an  $I = 0$  state, i.e., the  $\omega$  exchange channel. In this section, I will estimate the modification of this strength in the chiral limit. The change is very slight, and the net effect on nuclear binding is so small that it is well below even the uncertainty of the result in the scalar channel. The reason for this is clear: the  $3\pi$  channel is very small at threshold, and hence the threshold sensitivity that the scalar channel exhibited is absent. The chiral modification has the natural size of order  $m_\pi^2/(1\text{GeV})^2$ .

In the dispersion relation

$$G_V = \frac{2}{\pi} \int_{3m_\pi}^{\infty} \frac{d\mu}{\mu} \rho_V(\mu^2), \quad (28)$$

the spectral function  $\rho_V(\mu^2)$  is small at low energy. In chiral perturbation theory, it arises first as the cut in a

two-loop diagram and hence is higher order in the energy expansion. There is also a kinematic suppression since the three pions are in a total spin-one state. Both theoretically and phenomenologically there seems to be little strength in this channel, see, e.g., Ref. [35], until one reaches the energy of the  $\omega(783)$ , which is a narrow resonance coupled essentially entirely to three pions. After the  $\omega(783)$ , there is not another three-pion resonance until well over 1 GeV. It is then a reasonable approximation to take the vector spectral function dominated by the narrow resonance  $\omega(783)$ .

We need to understand how the properties of the  $\omega(783)$ , i.e., its mass and coupling, are modified in the chiral limit. We can estimate its mass in the chiral limit from the SU(3) breaking in the other vector mesons. Replacing one of the light quarks by a strange quark yields the  $K^*(890)$ , and replacing two of them produces the  $\phi(1040)$ . The vector mesons empirically obey an equal spacing rule. This leads to a simple linear interpolation formula as a function of the light quark mass  $\hat{m}$ :

$$m_V = m_\omega + (m_\phi - m_\omega) \frac{\hat{m} - \hat{m}_{\text{phys}}}{m_s - \hat{m}_{\text{phys}}}. \quad (29)$$

The chiral limit is found with  $\hat{m} = 0$ , resulting in

$$m_{\text{chiral}} = 783 - (1040 - 783) \frac{\hat{m}_{\text{phys}}}{m_s - \hat{m}_{\text{phys}}} = 770. \quad (30)$$

This is a 2% shift in the mass.

One can address the quark mass dependence of the vector coupling to nucleons again through the SU(3) breaking pattern plus data. The SU(3) breaking of the NNV couplings themselves is not known well enough experimentally to be of direct use. However, an indirect method can be employed. A phenomenologically successful model for these coupling, called vector meson dominance (VMD), relates the nucleon's NNV coupling  $g_v$  to the coupling of the vector meson to a photon  $f_v$ , defined via

$$\langle V | J_\mu | 0 \rangle = c_v f_v m_V^2 \epsilon_\mu, \quad (31)$$

where  $J_\mu$  is the electromagnetic current and  $c_v$  are known Clebsch-Gordon coefficients. The VMD relation is simply  $g_v = f_v^{-1}$  and can be motivated/derived from a dispersion relation argument for the electromagnetic current of the nucleon. Phenomenologically, VMD works very well. Since there is experimental evidence on the SU(3) breaking of  $f_v$ , we can use that plus VMD as an estimate of the quark mass dependence of  $g_v$ . I have performed a fit to the data involving the neutral vector mesons  $\rho$ ,  $\omega$ , and  $\phi$ , again assuming a linear interpolation. The result is a dependence of the form

$$g_v = g_{v0} [1 + b_{gv} (m_\pi^2 - m_{ph}^2)], \quad (32)$$

with  $b_{gv} = 0.57 \pm 0.22 \text{ GeV}^{-2}$ . The error bar comes from using different data in the evaluation of the SU(3) breaking. The central estimate is then

$$\frac{g_v|_{\text{chiral}}}{g_v|_{\text{physical}}} = 0.99. \quad (33)$$

We can combine the vector mass and coupling to determine the shift in the parameter vector coupling  $G_V = g_V^2/m_V^2$ . This

yields

$$\eta_{V,\text{ch}} \equiv \frac{G_V|_{\text{chiral}}}{G_V|_{\text{physical}}} = 0.995 \pm 0.020. \quad (34)$$

The variation of both the mass and the coupling constant were mild compared to the dependence that we have estimated for the scalar channel. Moreover, both the mass in the denominator and the coupling constant in the numerator decreased, leading to a very small net effect in the ratio. The error bar quoted is a generous estimate. In any case, the uncertainty in this coupling is significantly smaller than that in the scalar coupling.

## VIII. ESTIMATE OF THE CHANGES IN NUCLEAR BINDING ENERGY

Our results clearly have the strength of the attractive scalar coupling being significantly increased in the chiral limit. As I argued in Sec. II, in effective field theory the most consistent procedure would be to treat the long-range components of the two-pion exchange dynamically, most likely with a form of a cutoff, and then add the contact interactions to account for the rest of the interaction. This has not yet been done for heavy nuclei. However, the use of the contact interactions in point-coupling calculations of binding provide an estimate of the shift in the binding that is appropriate for the present state of the art.

Not all possible contact interactions play a significant role in nuclear binding. The dominant ingredients in the binding of heavy nuclei have been elucidated by Furnstahl, Serot, and coworkers [26,46]. The results can be extracted from Figs. 1 and 2 of [46]. It is clear that the dominant effects are the scalar and vector contributions, to the leading power of the density. Other interactions play reduced roles, although for a complete understanding of the binding, about a half-dozen contact interactions are required. I will consider only the dominant isoscalar-scalar and isoscalar-vector interactions; in practice, it is only the scalar coupling that has a significant dependence on the pion mass.

Using Ref. [46], one can read off the effects of the different contact terms.<sup>8</sup> I parametrize the results in terms of the strengths of the contact interactions, normalized to their physical values, defining

$$\begin{aligned} \eta_S &= \frac{G_S}{G_S|_{\text{physical}}}, \\ \eta_V &= \frac{G_V}{G_V|_{\text{physical}}}. \end{aligned} \quad (35)$$

The contributions to the binding energy numbers for  $^{16}\text{O}$  (in MeV) are

$$\frac{\text{B.E.}}{A} \sim -82\eta_S + 44\eta_V + 30. \quad (36)$$

The first two terms are the effects of the scalar- and vector-isoscalar interactions. The third term is the sum of four other

<sup>8</sup>I thank Dick Furnstahl and Brian Serot for assistance in understanding these numbers.

smaller contributions to the binding energy and kinetic energy contributions. There is, in addition, the Coulomb energy and a small center-of-mass correction. For  $^{208}\text{Pb}$ , the result is

$$\frac{\text{B.E.}}{A} \sim -104\eta_S + 57\eta_V + 36. \quad (37)$$

The results of these calculations can be generalized to other nuclei by a parametrization that resembles the semiempirical mass formula. For local interactions, because the nuclear density is nearly constant in the central region, one expects that the binding energy will have a dependence volume, which in turn is proportional to the number of particles  $r^3 \sim A$ , and that interactions that occur near the nuclear surface would have a modified result proportional to the number of nucleons near the surface,  $r^2 \sim A^{2/3}$ . This suggests that binding effects can be parametrized in terms of behavior in  $A$  and in  $A^{2/3}$ . Using the results for nuclear matter and for specific nuclei, we find a good fit of the form

$$\frac{\text{B.E.}}{A} = -\left(120 - \frac{97}{A^{1/3}}\right)\eta_S + \left(67 - \frac{57}{A^{1/3}}\right)\eta_V + \text{residual terms.} \quad (38)$$

Our results from the previous sections can be summarized as

$$\begin{aligned} \eta_{S,\text{ch}} &= \frac{G_S|_{\text{chiral}}}{G_S|_{\text{physical}}} = 1.37 \pm 0.10, \\ \eta_{V,\text{ch}} &= \frac{G_V|_{\text{chiral}}}{G_V|_{\text{physical}}} = 0.995. \end{aligned} \quad (39)$$

These numbers produce

$$\frac{\text{B.E.}}{A}|_{\text{chiral}} = -38 \pm 8 \text{ MeV} \quad (40)$$

for  $^{16}\text{O}$ , compared to the physical result of  $-8 \text{ MeV}$ . For  $^{208}\text{Pb}$ , the corresponding results are  $-49 \pm 10 \text{ MeV}$  in the chiral limit compared to  $-11 \text{ MeV}$  in the physical case. Finally, for the general parametrization, the results suggest a shift in the binding energy

$$\Delta \frac{\text{B.E.}}{A}|_{\text{chiral}} = -\left(44 - \frac{36}{A^{1/3}}\right). \quad (41)$$

These shifts are larger than we would naively expect. There are two ingredients in generating this magnitude. First is the large shift in the scalar contact interaction  $G_S$ . I have explained at length above why this large shift occurs and why it should be considered natural. The other ingredient is that there is a strong cancellation between the scalar and vector terms in the expression for the binding energy. The usual  $10 \text{ MeV/nucleon}$  binding energy is the difference of two significantly larger numbers. This is understandable from the meson exchange potential description. Scalar exchange provides a strong attractive potential. Vector meson exchange provides the repulsive short-range interaction and tends to oppose binding. The fact that the  $10 \text{ MeV}$  of binding energy is far below all other hadronic scales of QCD comes from the competition of these two opposing effects. When we go to the chiral limit and make the attractive interaction significantly stronger while leaving the repulsive one unchanged, the near

cancellation between these competing effects becomes less pronounced and the percentage shift is large.

## IX. THE CHIRAL SLOPE PARAMETER

Another way to present the results of this calculation is as the slope in the scalar coupling as one deviates from the chiral limit. The leading terms in an expansion around the chiral limit are given by

$$G_S = G_{S0}(1 + d_S m_\pi^2) + F_S m_\pi^3 + \dots, \quad (42)$$

where  $G_{S0}$  is the result in the chiral limit, and the nonanalytic term is [21]

$$F_S = -\frac{3g_A^2}{16\pi F_\pi^4}(6c_1 - 5c_3). \quad (43)$$

The effect of the  $F_S$  term is relatively small, i.e.,  $F_S m_\pi^3 / G_{S0} \sim 0.09$ .

It should be pointed out that the dispersion relation does not exactly reproduce the correct  $m_\pi^3$  dependence of the chiral coupling. The cubic mass dependence arises in the dispersive calculation from the threshold behavior of the chiral amplitude. Use of the chiral representation for the spectral function given in Eq. (18) leads to a cubic term that is

$$F_S^{(\text{disp})} = -\frac{3g_A^2}{16\pi F_\pi^4} \left(6c_1 - \frac{11}{3}c_3\right). \quad (44)$$

I checked both the spectral function and the real part of the loop calculation. This has nothing to do with the unitarization procedure and cannot be changed by higher order corrections to the threshold behavior. While the effect is numerically small, it represents a puzzle to which I do not understand the resolution.<sup>9</sup> It is fortunate that this nonanalytic term is numerically small and the effect of the disagreement has only a 2% effect on the determination of the slope.

I extracted the chiral slope by evaluating of the dispersion integral at several values of the pion mass and performing a fit using terms in  $m_\pi^2$  and  $m_\pi^4$  as well as the known nonanalytic term in  $m_\pi^3$ . The result of the fit yields the slope

$$d_S = -(17 \pm 5) \text{ GeV}^{-2} = -\frac{0.31 \pm 0.08}{m_\pi^2}. \quad (45)$$

The negative sign is indicative of the the fact that the scalar coupling is smaller in the physical case than it is in the chiral limit. This slope is relatively large for the reasons discussed above. Again, because the ratios of scalar couplings are predicted better than the absolute values, the parameter  $d_S$  is much better determined in this calculation than  $D_S \equiv d_S G_{S0}$ . As seen in the previous section, the slope of the combination of the two isoscalar effects in the overall nuclear central force is yet larger because of the partial cancellation of the scalar and vector channels.

<sup>9</sup>I thank E. Epelbaum, U. Meißner, N. Kaiser, and Barry Holstein for discussions about this issue.

## X. SUMMARY AND DISCUSSION

I have used the chiral results for the low-energy behavior of the dispersion relation for the scalar contact interaction, supplemented with a representation for the Omnes function, in order to calculate the strength of the central nuclear force in the chiral limit. In the results, the largest modifications are seen to come from the low-energy amplitudes, which extend down to zero energy in the chiral case. While there are some uncertainties in the final result, most notably from the uncertainty in the chiral extrapolation of  $g_A$ , the key ingredients in the calculation appear clear. We also understand qualitatively why the effect is relatively large.

Since this has been an attempt to calculate the full scalar coupling, I have had to model the high-energy contributions. While I have argued that this modeling has not introduced large effects in the final results, there is also a way to use this method with the full rigor of chiral perturbation theory. To do this, one would use the present calculation dynamically and in addition introduce a residual contact interaction to account for high-energy effects which have been misrepresented in the present calculation. This extra parameter would presumably be small and would not be expected to have much mass variation. This variant of the Wilsonian scheme described in Sec. II would then be a way to implement the effective field theory treatment while capturing the main dynamical results of the present calculation.

Several other works discuss nuclear interaction in the chiral limit [4–6] within the context of chiral perturbation theory. The present work is different because it is a dynamical attempt to

calculate the mass variation in the scalar channel. Previous work has been both more general, because this variation was parametrized a chiral coefficient, and more limited, because this coefficient could only be guessed at. In practice, the mass variation found in this paper is larger than the estimates of [4,5] and has a well-determined sign. Another difference is that the previous works focused on few-nucleon systems. This requires the addition of single-pion exchange, which obviously also has a significant change in the chiral limit. My contribution here is only on the scalar sector, hence I have limited my comments on binding to the heavy nuclear case for which one-pion exchange is not important. However, it is clear that the results of this paper would push the binding of few-nucleon systems in the direction of *greater* binding. It would be interesting to revisit the few-nucleon case with either the parameter  $d_S$  calculated in the present work or with a full Wilsonian treatment dynamically including the effects of low-energy two-pion exchange.

## ACKNOWLEDGMENTS

I especially thank Thibault Damour for many conversations during the course of this work. In addition, I have benefited from discussions with U. van Kolck, R. Furnstahl, B. Serot, E. Epelbaum, U. Meißner, N. Kaiser, and Barry Holstein. I also appreciate the hospitality of the IHES where most of this work was performed. This work has been partially supported by the U.S National Science Foundation.

- 
- [1] W. Cottingham and R. Vinh Mau, Phys. Rev. **130**, 735 (1963); W. N. Cottingham, M. Lacombe, B. Loiseau, J. M. Richard, and R. Vinh Mau, Phys. Rev. D **8**, 800 (1973).
  - [2] M. Chemtob, J. W. Durso, and D. O. Riska, Nucl. Phys. **B38**, 141 (1972).
  - [3] J. F. Donoghue, arXiv:nucl-th/0602074.
  - [4] E. Epelbaum, U. G. Meißner, and W. Glöckle, Nucl. Phys. **A714**, 535 (2003); E. Epelbaum, U. G. Meißner, and W. Glöckle, arXiv:nucl-th/0208040.
  - [5] S. R. Beane and M. J. Savage, Nucl. Phys. **A717**, 91 (2003); **A713**, 148 (2003).
  - [6] U. G. Meißner, Proceedings of Science LAT2005, 009 (2005) [arXiv:hep-lat/0509029].
  - [7] K. G. Wilson and J. B. Kogut, Phys. Rep. **12**, 75 (1974).
  - [8] R. F. Dashen, Phys. Rev. **183**, 1245 (1969).
  - [9] J. Bijnens, Phys. Lett. **B306**, 343 (1993); J. Bijnens and J. Prades, Nucl. Phys. **B490**, 239 (1997); J. F. Donoghue, B. R. Holstein, and D. Wyler, Phys. Rev. D **47**, 2089 (1993); J. F. Donoghue and A. F. Perez, *ibid.* **55**, 7075 (1997).
  - [10] T. Das, G. S. Guralnik, V. S. Mathur, F. E. Low, and J. E. Young, Phys. Rev. Lett. **18**, 759 (1967).
  - [11] V. Cirigliano, J. F. Donoghue, E. Golowich, and K. Maltman, Phys. Lett. **B522**, 245 (2001).
  - [12] E. Epelbaum, W. Glöckle, and U. G. Meißner, Eur. Phys. J. A **19**, 125 (2004); **19**, 401 (2004).
  - [13] U. G. Meißner, Nucl. Phys. **A751**, 149 (2005).
  - [14] G. E. Brown and A. D. Jackson, *The Nucleon-Nucleon Interaction* (North-Holland, Amsterdam, 1977).
  - [15] T. E. O. Ericson and W. Weise, *Pions and Nuclei* (Clarendon, Oxford, 1988).
  - [16] E. Epelbaum, Ulf-G. Meißner, W. Glöckle, and C. Elster, “Resonance saturation for four-nucleon operators,” Phys. Rev. C **65**, 044001 (2002).
  - [17] C. Ordóñez and U. van Kolck, Phys. Lett. **B291**, 459 (1992); C. Ordóñez, L. Ray, and U. van Kolck, Phys. Rev. C **53**, 2086 (1996); J. L. Friar and U. van Kolck, *ibid.* **60**, 034006 (1999).
  - [18] S. R. Beane, P. F. Bedaque, W. C. Haxton, D. R. Phillips, and M. J. Savage, From hadrons to nuclei: Crossing the border,” arXiv:nucl-th/0008064, published in *At the frontier of particle physics*, edited by M. Shifman (World Scientific, 2001), Vol. I, pp. 133–269.
  - [19] P. F. Bedaque and U. van Kolck, Annu. Rev. Nucl. Part. Sci. **52**, 339 (2002).
  - [20] E. Epelbaum, Prog. Part. Nucl. Phys. **57**, 654 (2006).
  - [21] N. Kaiser, R. Brockmann, and W. Weise, Nucl. Phys. **A625**, 758 (1997).
  - [22] N. Kaiser, Phys. Rev. C **64**, 057001 (2001); D. R. Entem and R. Machleidt, *ibid.* **66**, 014002 (2002).
  - [23] N. Kaiser, Phys. Rev. C **65**, 017001 (2002); **61**, 014003 (2000); **62**, 024001 (2000); **63**, 044010 (2001).
  - [24] T. Becher and H. Leutwyler, Eur. Phys. J. C **9**, 643 (1999).
  - [25] R. Higa and M. R. Robilotta, Phys. Rev. C **68**, 024004 (2003).

- [26] B. D. Serot and J. D. Walecka, in *150 year of Quantum Many-Body theory*, edited by R. F. Bishop, K. A. Gernoth, and N. R. Walet (World Scientific, Singapur, 2001), p. 203; *Int. J. Mod. Phys. E* **6**, 515 (1997); J. J. Rusnak and R. J. Furnstahl, *Nucl. Phys. A* **627**, 495 (1997).
- [27] R. Omnes, *Nuovo Cimento* **8**, 316 (1958).
- [28] J. F. Donoghue, J. Gasser, and H. Leutwyler, *Nucl. Phys. B* **343**, 341 (1990).
- [29] J. Gasser and H. Leutwyler, *Ann. Phys. (NY)* **158**, 142 (1984).
- [30] G. Colangelo, J. Gasser, and H. Leutwyler, *Nucl. Phys. B* **603**, 125 (2001).
- [31] A. Dobado and J. R. Pelaez, *Phys. Rev. D* **56**, 3057 (1997); T. N. Truong, *Phys. Rev. Lett.* **67**, 2260 (1991).
- [32] J. A. Oller and E. Oset, *Phys. Rev. D* **60**, 074023 (1999).
- [33] J. Gasser and U. G. Meißner, *Nucl. Phys. B* **357**, 90 (1991).
- [34] N. Fettes, U. G. Meißner, and S. Steininger, *Nucl. Phys. A* **640**, 199 (1998); N. Fettes, U. G. Meißner, M. Mojzisz, and S. Steininger, *Ann. Phys. (NY)* **283**, 273 (2000); **288**, 249 (E) (2001); S. Steininger, U. G. Meißner, and N. Fettes, *J. High Energy Phys.* 09 (1998) 008; J. Kambor and M. Mojzisz, *J. High Energy Phys.* 04 (1999) 031.
- [35] V. Bernard, N. Kaiser, and U. G. Meißner, *Nucl. Phys. A* **615**, 483 (1997); **A611**, 429 (1996) [arXiv:hep-ph/9607428].
- [36] M. C. M. Rentmeester, R. G. E. Timmermans, J. L. Friar, and J. J. de Swart, *Phys. Rev. Lett.* **82**, 4992 (1999) [arXiv:nucl-th/9901054]; *Phys. Rev. C* **67**, 044001 (2003).
- [37] I. Caprini, G. Colangelo, and H. Leutwyler, *Phys. Rev. Lett.* **96**, 132001 (2006).
- [38] R. Vinh Mau, J. M. Richard, B. Loiseau, M. Lacombe, and W. N. Cottingham, *Phys. Lett. B* **44** 1 (1973); W. N. Cottingham, M. Lacombe, B. Loiseau, J. M. Richard, and R. Vinh Mau, *Phys. Rev. D* **8** 800 (1973); R. Vinh Mau, *Lect. Notes Phys.* **581** 1 (2001).
- [39] R. Rapp, J. W. Durso, and J. Wambach, *Nucl. Phys. A* **615**, 501 (1997) [arXiv:nucl-th/9611019].
- [40] K. Holinde, *Prog. Part. Nucl. Phys.* **36**, 311 (1996); *Nucl. Phys. A* **543**, 143c (1992); C. Schutz, J. W. Durso, K. Holinde, and J. Speth, *Phys. Rev. C* **49**, 2671 (1994); H. C. Kim, J. W. Durso, and K. Holinde, *ibid.* **49**, 2355 (1994).
- [41] V. G. J. Stoks, R. A. M. Klomp, C. P. F. Terheggen, and J. J. de Swart, *Phys. Rev. C* **49**, 2950 (1994).
- [42] U. G. Meißner, *Comments Nucl. Part. Phys.* **20**, 119 (1991).
- [43] W. Grein and P. Kroll, *Nucl. Phys. A* **338**, 332 (1980).
- [44] E. Oset, H. Toki, M. Mizobe, and T. T. Takahashi, *Prog. Theor. Phys.* **103**, 351 (2000).
- [45] F. Wang, G. H. Wu, L. J. Teng, and T. Goldman, *Phys. Rev. Lett.* **69**, 2901 (1992); G. H. Wu, L. J. Teng, J. L. Ping, F. Wang, and T. Goldman, *Commun. Theor. Phys.* **22**, 449 (1994); *Mod. Phys. Lett. A* **10**, 1895 (1995); H. R. Pang, J. L. Ping, F. Wang, and T. Goldman, *Phys. Rev. C* **65**, 014003 (2002).
- [46] R. J. Furnstahl and B. D. Serot, *Nucl. Phys. A* **671**, 447 (2000).